Supplementary materials

1. Finite element analysis method[s1]:

We Used the Mooney-Rivlin model. The strain potential energy of this model is defined as:

$$W = C_{10}\left(\bar{I}_1 - 3\right) + C_{01}\left(\bar{I}_2 - 3\right) + \frac{1}{d}\left(J-1\right)^2 \tag{S1}$$

Where: W is the strain potential energy function; $\bar{I}_1$ is the first strain excursion invariant; $\bar{I}_2$ is the second strain excursion invariant; and C_{10}, C_{01} are the material constants; d is the material incompressibility parameter; J is the relevant parameter.

The initial shear modulus is defined as:

$$\mu = 2\left(C_{10} + C_{01}\right) \tag{S2}$$

The initial bulk modulus is defined as:

$$k = \frac{2}{d} \tag{S3}$$

Where:

$$C_{10} = \frac{E}{5\left(1+\nu\right)} \qquad C_{01} = \frac{E}{20\left(1+\nu\right)} \qquad d = \frac{6\left(1-2\nu\right)}{E} \tag{S4}$$

Where: E is the elastic modulus of the material (see components A and B in Table 3); ν is the Poisson's ratio of the material.

The above analysis is mainly summarized as the analysis of the desorption between the two interfaces initially bonded to each other. Therefore, it is suitable to use the cohesion model for the above analysis, and the involved cohesion surface can be used to simulate a wider range of cohesive interactions. For example, it is used to analyze the situation where two sticky surfaces are in contact during the process. The cohesive force surface model expresses the complex failure process between two surfaces with a "Traction-separation-based modeling". The cohesive surface model that comes with ABAQUS is a linear triangular model (bilinear constitutive model), which assumes that the avulsion process is initially a linear elastic behavior, followed by the initiation and evolution of damage.

Linear elastic behavior is represented by an elastic constitutive matrix, which establishes the relationship between the normal and tangential stresses at the interface and the corresponding normal and tangential separations.

$$\sigma = \begin{Bmatrix} \sigma_n \\ \sigma_s \\ \sigma_t \end{Bmatrix} = \begin{bmatrix} K_{nn} & K_{ns} & K_{nt} \\ K_{ns} & K_{ss} & K_{st} \\ K_{nt} & K_{st} & K_{tt} \end{bmatrix} \begin{Bmatrix} \varepsilon_n \\ \varepsilon_s \\ \varepsilon_t \end{Bmatrix} = K\varepsilon \tag{S5}$$

where σ is the traction stress vector, which consists of three parts, including a normal traction stress σ_n and two tangential traction stresses σ_s and σ_t; K represents the stiffness coefficient matrix.

Damage initiation refers to the onset of degradation of cohesive behavior in the contact area, and the degradation process begins when contact stress and/or contact separation satisfy certain specified damage initiation conditions. There are two main types of evaluation criteria for damage initiation: maximum stress criterion and maximum strain criterion. In this paper, the maximum nominal stress criterion is chosen as the criterion for evaluating damage initiation.

$$\max\left\{\frac{\langle\sigma_n\rangle}{\sigma_n^o},\quad \frac{\sigma_s}{\sigma_s^o},\quad \frac{\sigma_t}{\sigma_t^o}\right\}=1 \tag{S6}$$

The damage is assumed to start when the maximum contact stress ratio (as defined by the expression) reaches 1. Where $\sigma_n^o, \sigma_s^o, \sigma_t^o$ represent the peak value of the contact stress at the contact point when the separation direction is completely perpendicular to the interface or completely along the first tangential direction or completely along the second tangential direction, respectively. σ_n, σ_s, σ_t are the actual stress in the three directions, and the symbol Macaulay bracket $\langle\ \rangle$ indicates that pure compressive displacement or pure compressive stress state will not cause damage.

The cohesive surface model (bilinear constitutive model) based on the maximum nominal stress fracture criterion is shown in Appendix Figure 1, where the AB segment represents the initial linear elastic behavior, and the slope is the material stiffness. Point B is the starting point of damage, and the stress at point B is the peak stress that the interface can withstand in a single direction. Segment BC is the process of damage evolution, and point C is the failure point. The shaded part in the figure represents the interface fracture energy.

During the simulation process, a plane simplified model is established, and the lower parting surface is fixed, while the upper parting surface is displaced along the vertical direction until they are completely separated. In this process, the lower parting surface is coupled to a point, and the contact reaction force RF at this point in the whole separation process is extracted, which is the interface separation force between the parting surfaces. According to the bilinear constitutive model introduced in the support material, the area, which is enclosed by the change curve of the interface separation force of the parting surface and the horizontal axis, is the avulsion energy generated between the parting surfaces. For details, see Appendix Figure 1.

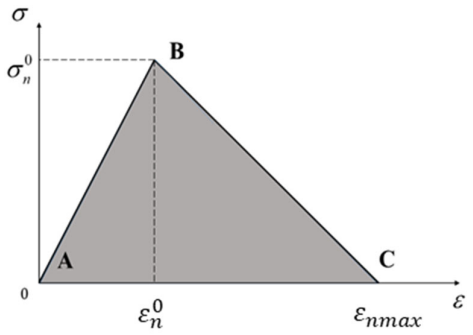

Figure S1 Bilinear Constitutive Model

2. Orthogonal test method:

For the safety of the tenon part, some parameter relationships of the dovetail tenon structure are as follows[s2]:

$$\frac{1}{5} \le W/H \le \frac{2}{3} \qquad W < W_t \le \frac{2H}{3} \tag{S7}$$

The overall length H is 6mm, so three levels of W, H_t and W_t are set as shown in Table S1. Therefore, there are 27 kinds of combination comparisons. In order to reduce the number of combination comparisons, we decided to use the orthogonal experiment method to extract representative combinations for comparison. The specific orthogonal experiment table is shown in Table 1. According to the 9 horizontal combination methods in Table 1, the simulation avulsion analysis was carried out in turn, and the avulsion state of each of the 9 combination methods at the same avulsion moment and the interfacial separation force and avulsion energy during the whole separation process were also compared.

Table S1 Three factors and their corresponding levels

		Factors		
		W	H_t	W_t
Levels	1	1.5 mm	1.5 mm	3 mm
	2	2 mm	2 mm	3.5 mm
	3	2.5 mm	2.5 mm	4 mm

3. Calculations related to mold design

According to the calculation formula of the shrinkage rate of rubber:

$$S_{CP} = \frac{V_1 - V_2}{V_1} \times 100\% \tag{S8}$$

Where S_{CP} (%) is the average shrinkage of rubber; V_1 (cm^3) is the volume of the mold cavity; V_2 (cm^3) is the volume of rubber products.

Considering that the production curing temperature is 100°C, the shrinkage rate of Dow Corning SYLGARD 184 is calculated to be 9.6% by testing at 100°C.

According to the size formula of the rubber mold cavity：

$$D_M = \left[\left(1 + S_{CP}\right) \times D_Z \pm \frac{\Delta_Z}{2} \right] \pm \Delta_M \tag{S9}$$

Where D_M (mm) is the size of the mold cavity; D_Z (mm)is the size of the produc; S_{CP} (%) is the average shrinkage of rubber; Δ_Z (mm)is tolerances on product dimensions; Δ_M (mm) is manufacturing tolerances for mold cavities。

The specific design size of the product is shown in Appendix Fig 2; the dimensional tolerance of the mold product spans two intervals (+) and (-), and it is symmetrically distributed, so Δ_Z is taken as zero; Since the mold material is 7500 high-performance nylon resin from Future Factory, it can be seen that the manufacturing tolerance of the mold cavity Δ_M is 0.2mm.

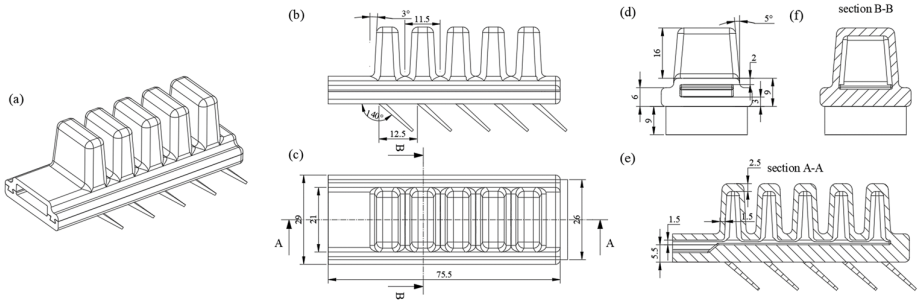

Figure S2 The specific design size of the product: (a) isometric view; (b) front view; (c) top view; (d) left view; (e) Section A-A; and (f) Section B-B.

The calculation of the size of the mold cavity can be carried out according to the above parameters. For example, the cavity size corresponding to a length of 75.5mm is as follows：

$$\begin{aligned} D_M &= \left[\left(1 + S_{CP}\right) \times D_Z \pm \frac{\Delta_Z}{2} \right] \pm \Delta_M \\ &= \left[\left(1 + 9.6\%\right) \times \left(75.5\right) \pm 0 \right] \pm 0.2\text{mm} \\ &= 82.748 \pm 0.2\text{mm} \end{aligned}$$

It is known that the length of the entire mold cavity is 82.748±0.2mm. This data is used to guide the design of the mold, and the remaining dimensions can be calculated in sequence according to this step.

4. Instructions for use of the pneumatic drive system

The two-way pneumatic drive system (Figure 7a and 7b) uses a pneumatic source (the output air pressure range is 0~700 kPa, and the output flow is 0~40 L/min) to provide pressure for the positive and negative air pressure circuits. Each circuit is connected in series with a solenoid valve that acts as a switch, which is opened when the circuit enters the working state, and is closed in the other states (at most one circuit is in the working state at the same time). The positive air pressure

circuit realizes the linear control of air pressure through the series electric proportional valve (SMC-ITV-1050), and the negative air pressure circuit generates negative pressure through the series vacuum generator. The two circuits are finally combined into one output terminal and connected to Bio-AU. The positive air pressure output by the air pressure drive system is in the range of 0~150 kPa, while the absolute value of the negative air pressure output by the air pressure drive system is the same as the positive air pressure output by the air pump, and the output air pressure of the negative air pressure circuit can be controlled by changing the output air pressure of the air pump. The error of the output air pressure value of the whole air drive system is ±2 kPa. The whole system has fast driving speed and high switching efficiency. All components are controlled by Arduino nano, which can realize the inflatable expansion and inspiratory contraction of the bionic toe within 0.2s respectively.

S-References:

s1. Wang, Liuwei. *Design of Bionic Flexible Autonomous Adhesion-Desorption Unit and Adhesion Grasping Device*; Nanjing University of Aeronautics and Astronautics: Nanjing, China, 2019.

s2. Yang, Jianfu. *Influence of Tenon-Mortise Structural Parameters On its Mechanical Propertie*; Beijing University of Technology: Beijing, China, 2017.